# Linear-least-squares fitting method for the solution of the time-dependent Schrödinger equation: Applications to atoms in intense laser fields

Xiaoxin Zhou[1,2] and C. D. Lin[1]
[1]*Department of Physics, Kansas State University, Manhattan, Kansas 66506-2601*
[2]*Department of Physics, Northwest Normal University, Lanzhou, Ganzu, 730070, People's Republic of China and Wuhan Institute of Physics, Chinese Academy of Sciences, Wuhan, 430071, People's Republic of China*
(Received 7 October 1999; published 18 April 2000)

An alternative theoretical approach for solving the time-dependent Schrödinger equation for atoms in an intense laser field is presented. In this method the time-dependent wave function is expanded in a basis set but the expansion coefficients are determined by linear-least-squares fitting of the wave function on discrete mesh points in configuration space, thus avoiding the need of evaluating a large number of matrix elements. We illustrate the method by computing wave functions, above-threshold ionization spectra, and harmonic generation spectra of a model atom and compare the results with those obtained using the split-operator method.

PACS number(s): 42.50.Hz, 32.80.Qk, 32.80.Rm, 32.80.Wr

## I. INTRODUCTION

When atoms are exposed to an intense laser field, multiphoton phenomena such as the above-threshold ionization (ATI) and harmonic generation (HG) have been observed in experiments [1–3]. In order to describe these phenomena theoretically, perturbative approaches are not useful when the laser field strength is comparable to the atomic field. Among the nonperturbative methods that are commonly used, the important ones are the Floquet theory [4,5], the direct solution of the time-dependent equation on numerical grid points [6–10], and the basis set expansion method. In the basis set expansion method, the time-dependent wavefunction is expanded in some basis set and the problem is reduced to the solution of a set of coupled first-order differential equations in time. The basis functions that have been used so far include the set of field-free bound and continuum states [11–13], a set of states generated from the *B* splines [14] or the set of Sturmian functions [15,16]. In other cases, Volkov states which are eigenstates of a free electron in a laser field have also been used as basis functions [17]. The basis function approach in general can be tailored more directly to the physical problems on hand, however, it does require the evaluation of a large number of matrix elements which is very time consuming, especially those elements between continuum states. Solving the time-dependent problem on the numerical grids would avoid the need of evaluating matrix elements. However, the accurate representation of a rapidly oscillating function requires relatively dense grid points and thus memory and CPU requirement becomes substantial.

From the mathematical viewpoint the interaction between an intense laser field with atoms is not very different from the interaction of a charged particle with atoms in that one has to solve the time-dependent Schrödinger equation nonperturbatively. In general the theory of ion-atom collisions is perceived as more difficult because of the two-center nature, where one needs to describe charge transfer processes in addition to the excitation and ionization processes. For atoms in a laser field, it is perceived as simpler because it is a single-center problem. This perception is correct if the ''laser'' is a half-cycle pulse [18] (or quarter-cycle pulse [19]), but not when it is a long pulse consisting of many cycles. In a longer pulse the electron experiences many back-and-forth oscillations of the laser field, resulting in complicated interference of the electronic wavefunctions which are not easily expanded in a small set of basis functions. The representation of the wavefunction of an atomic electron in a laser field in general requires a larger primitive basis set, much larger than those employed normally in ion-atom collisions.

The perception of the success of the basis set expansion method in ion-atom collisions in fact is misguided. It is due mostly to the lack of detailed experimental studies of the momentum distributions of the ionized electrons so far, especially at lower energies. In recent years, with the advent of the COLTRIMS apparatus [20,21], detailed ejected electron momentum distributions have been measured and the limitation of the basis set expansion method became apparent. New theoretical approaches have to be developed in order to address the electron momentum distributions. In the method of Sidky and Lin [22], the time-dependent wavefunction is expanded in basis functions in momentum space. The propagation of the wavefunction is carried out in configuration space where the expansion coefficients, instead of being found by solving the coupled equations as in the standard approach, were obtained by a linear-least-squares fitting procedure on a set of grid points. When the number of grid points goes to infinity the result of the linear-least-squares fitting procedure is formally identical to solving the close-coupling equations exactly. However, the goal of the linear-least-squares fitting method is to solve a large set of coupled equations approximately. Clearly this method offers no advantages if the number of coupled equations is small since one may just solve the coupled equations exactly. On the other hand, there are situations where one intrinsically has to deal with a large number of coupled equations. Exact solution of such close-coupling equations would be rather time consuming and impractical. With the fitting procedure, it is anticipated that the large number of coupled equations can be

 ©2000 The American Physical Society

solved approximately to certain degrees of accuracy. This alternative method is attractive since it removes the need of the most time-consuming part of evaluating matrix elements where the CPU requirement goes roughly with $N^3$ to $N^4$, where $N$ is the basis size. The fitting procedure is expected to increase roughly linearly with the basis size.

Above-threshold ionization and harmonic generation are fascinating observable phenomena in laser-atom collisions and they are easily calculated from theory once we can obtain accurate representation of the fast oscillating time-dependent electronic wave function. If the time-dependent wave function is to be expanded in some basis set, clearly continuum basis functions are needed in order to represent ionization. In such calculations, as stated before, the evaluation of matrix elements between continuum functions is rather problematic. If square-integrable basis functions are used, then reflected waves from the boundaries would produce complicated interference and introduce unphysical oscillations. To eliminate these interferences, one of the commonly used approaches is to introduce absorber near the boundaries to inhibit these reflections. For example, absorber are used in the split-operator methods [23].

Numerical methods which do not require the evaluation of matrix elements are often based on calculating the wave function at the grid points in configuration space. In order to be able to use efficient algorithms, the grid points in most cases are required to be equally spaced. This limits the flexibility of the method since fine-spaced meshes are needed to represent the atomic core region where the atomic potential changes rapidly, but relatively larger spaced meshes can be used to describe the ionized electron in the outer region where the potential is weak and flat.

In the present approach, the time-dependent electronic wavefunction in a laser field is expanded in a basis set. In solving the time-dependent equations for the expansion coefficients, however, we used a linear-least-squares fitting procedure. We will show how the ''accuracy'' of the fitting can be controlled by the basis functions and the range of the numerical integration or the ''box'' size. The fitting procedure can remove high-frequency interferences which tend to come from reflections at the boundaries. In fact, by choosing the basis functions judiciously the need of introducing absorber on the boundaries can be avoided.

The rest of this paper is arranged as follows. In Sec. II we discuss the present numerical method tailored for the laser-atom collision system. The formulation will be limited to a one-dimensional problem but generalization to three-dimensional systems is straightforward. In Sec. III we present a number of test calculations and the results are compared to those obtained from the split-operator method. The latter method is considered to be well-established for the one-dimensional problem. Thus the present calculations are compared with the split-operator method results in order to establish the reliability of the fitting method. Our goal is to generalize the present method to full three-dimensional problems and to arbitrary fields and potentials. The harmonic generation spectra and the ATI spectra calculated for the model problem are used to show the validity of the present method. A short summary and discussion of the future extension of the method is given in Sec. IV.

## II. THEORETICAL METHODS

### A. Basic formulation

We consider a one-dimensional atom in a laser field. In the dipole approximation the time-dependent Schrödinger equation in the length gauge is (atomic units are used throughout this paper)

$$i\frac{\partial\psi(x,t)}{\partial t}=H(x,t)\psi(x,t), \tag{1}$$

where $H(x,t)$ is the full Hamiltonian

$$H(x,t)=-\frac{1}{2}\frac{d^2}{dx^2}+V(x)-x\epsilon(t), \tag{2}$$

and $V(x)$ is the model potential of the atom. In this paper we will consider the soft Coulomb potential [24]

$$V(x)=-\frac{1}{\sqrt{1+x^2}} \tag{3}$$

only in order to be able to compare with other theoretical results. In Eq. (2), $\epsilon(t)$ is the electric field of the the laser pulse. The time-dependent solution $\psi(x,t)$ can be expanded in a basis set

$$\psi(x,t)=\sum_{n=1}^{N} c_n(t)\varphi_n(x). \tag{4}$$

Substitution of Eq. (4) into Eq. (1) leads to

$$i\sum_{n=1}^{N}\frac{dc_n(t)}{dt}\varphi_n(x)=\sum_{n=1}^{N}H(x,t)c_n(t)\varphi_n(x). \tag{5}$$

The ''standard'' approach in solving Eq. (5) is to project it onto the basis functions $\varphi_n(x)$ to obtain a set of coupled first-order differential equations for $c_n(t)$. The number of matrix elements needed to be evaluated then is of the order of $N^2$ if $N$ is the size of the basis set. The first-order coupled equations are then integrated to obtain the expansion coefficients to extract the scattering amplitudes.

An alternative approach, as first employed by Sidky and Lin [22], is to solve Eq. (5) on the discretized space coordinate $x_\alpha$ ($\alpha=1,2,\ldots,M$). Define the column matrices $\dot{C}$ and $A$, and a rectangular matrix $B$ by

$$\dot{C}=\begin{bmatrix} dc_1(t)/dt \\ dc_2(t)/dt \\ \cdots \\ dc_N(t)/dt \end{bmatrix} \quad B=\begin{bmatrix} \varphi_1(x_1) & \varphi_2(x_1) & \cdots & \varphi_N(x_1) \\ \varphi_1(x_2) & \varphi_2(x_2) & \cdots & \varphi_N(x_2) \\ \cdots & \cdots & \cdots & \cdots \\ \varphi_1(x_M) & \varphi_2(x_M) & \cdots & \varphi_N(x_M) \end{bmatrix} \quad A=\begin{bmatrix} \sum_n H(x_1,t)c_n(t)\varphi_n(x_1) \\ \sum_n H(x_2,t)c_n(t)\varphi_n(x_2) \\ \cdots \\ \sum_n H(x_M,t)c_n(t)\varphi_n(x_M) \end{bmatrix} \tag{6}$$

the resulting algebraic equations from (5) on the discretized points can be expressed as

$$i\sum_{n=1}^{N} B_{mn}\frac{dc_n(t)}{dt}=A_m, \quad m=1,2,\ldots,M \quad (M>N) \tag{7}$$

or in matrix form

$$i\,B\,\dot{C}=A. \tag{8}$$

The matrix $B$ is often called the design matrix. Since the number of equations $M$ is greater than the number $N$ of unknowns $[dc_n(t)/dt]$, this equation is overdetermined. Thus instead of searching for equality on the two sides of (7), we look for the least squares,

$$X=\sum_{m=1}^{M}\left|i\sum_{n=1}^{N} B_{mn}\frac{dc_n(t)}{dt}-A_m\right|^2. \tag{9}$$

The set of linear coefficients $[dc_n(t)/dt]$ which make $X$ the smallest then satisfy the equations (see Press *et al.* [25])

$$i\sum_{n'=1}^{N}\left(\sum_{m=1}^{M} B_{nm}B_{mn'}\right)\frac{dc_{n'}(t)}{dt}=\sum_{m=1}^{M} B_{nm}A_m \qquad n=1,2,\ldots,N. \tag{10}$$

In matrix form, this is

$$i(B^TB)\dot{C}=B^TA, \tag{11}$$

where $B^T$ is the transpose of $B$. Equation (11) is a set of $N$ algebraic equations of $N$ unknowns which can be solved directly. Thus the linear-least-squares fitting procedure provides a way to calculate $dc_n(t)/dt$ without the need of computing the matrix elements. It is understood that the method is an approximate solution to the coupled equations and one can show formally that as the number of discretized points goes to infinity, the fitting procedure gives the same results as the original coupled equations. Once the coefficients $c_i(t_0)(i=1,2,\ldots,N)$ are given at $t_0$, the best values of $dc_i(t_0)/dt$ are sought based on the data of $B$ and $A$ using the standard LU decomposition and back substitution procedure. After the time derivatives are obtained, the propagation to the next time step $c_i(t_0+\delta t)$ is straightforward. We used the fourth-order Runge-Kutta method.

This method allows us to integrate the time-dependent wave function $\psi(x,t)$ till the time when the laser pulse is turned off. Once the wave function is available, it is a simple matter to evaluate the following experimental quantities:

#### *1. Harmonic generation*

Harmonic-generation spectra are proportional to the modulus-squared of the Fourier transform $a(\omega)$ of the expectation value of the acceleration $a(t)$. By means of Ehrenfest's theorem,

$$a(t)=\langle\psi(x,t)|-\frac{x}{(1+x^2)^{3/2}}-\epsilon(t)|\psi(x,t)\rangle. \tag{12}$$

#### *2. ATI spectrum*

The ATI spectrum can be obtained by projecting the time-dependent wave function at $t=T_{final}$ onto the field-free continuum states $\phi_c^E(x)$,

$$P(E)=|\langle\varphi_c^E(x)|\psi(x,t=T_{final})\rangle|^2 \tag{13}$$

#### *3. Total ionization probabilities*

The total time-dependent ionization probability is defined as

$$P_{ion}(t)=1-\sum_{bound}|\langle\varphi_n(x)|\psi(x,t)\rangle|^2, \tag{14}$$

where the summation is over all the bound states $\varphi_n(x)$ when the field has been turned off.

### B. Basis set

To implement the present method we need to specify the basis functions and the range of the variable $x$ which is confined to $(-x_{max},+x_{max})$. In order to represent the continuum functions adequately it is desirable to have dense distribution of pseudostates. To this end each basis function is expanded as

$$\varphi_j(x)=\sum_{n=1}^{n_1} A_n\phi_n(x)+\sum_{n=1}^{n_2}\left[B_n\cos\left(\frac{n\pi x}{x_{max}}\right)+C_n\sin\left(\frac{n\pi x}{x_{max}}\right)\right], \tag{15}$$

where the $\phi_n(x)$ are the bound state wavefunctions of the field-free Hamiltonian, constructed from the *B*-spline basis, and the sine and cosine functions are members of a truncated Fourier series. The basis functions, $\varphi_j(x)$, with energy $E_j$, are obtained by diagonalizing the field-free Hamiltonian and thus are orthogonal. The energies of the lowest 20 eigenstates thus obtained are identical to those given by Eberly *et al.* [26]. The diagonalization also gives a spectrum of states where the energies are above the field-free threshold. These are the pseudostates and their density can be controlled by the size of the box.

The basis functions thus generated are then used to perform time-dependent calculations as outlined in the previous subsection.

### III. NUMERICAL RESULTS AND DISCUSSION

To illustrate the present numerical method we chose the one-dimensional (1D) model problem with the modified Coulomb potential Eq. (3) and laser field profile

$$\epsilon(t)=\begin{cases} E_0\sin^2\left(\dfrac{\pi t}{6T}\right)\sin\omega t, & 0\leqslant t\leqslant 3T \\ E_0\sin\omega t, & t>3T, \end{cases} \tag{16}$$

where $E_0$ is the amplitude of the laser field. First we consider these laser parameters: $E_0=0.1$ a.u., $\omega=0.148$ a.u. ($I=3.5\times10^{14}$ w/cm$^2$) and $T=2\pi/\omega$. At this frequency it takes about five photons to ionize the model atom from the ground state. In the calculation, the density of states, as seen from Eq. (15), is essentially determined by the interval $(-x_{max}, x_{max})$. For $x_{max}$ of the order of 150 a.u. the basis functions are adequate for a good fitting of the time-dependent wavefunction. In our calculations we typically take $n_1=3$, $n_2=200$, 300, and 400 for $x_{max}=200$, 300, and 400, respectively [see Eq. (15)]. Thus the maximum energy of the pseudostates is fixed roughly at 4.9 a.u. For the present soft Coulomb potential problem, we used equally-spaced grids of spacing of 0.3 or 0.4. The incremental step of the time-integration is 0.06 to 0.08. For the harmonic generation we propagate the time to 16 cycles and for the ATI to 16.25 cycles. The electron is initially in the ground state.

#### A. Results for $E_0=0.1$ a.u. and $\omega=0.148$ a.u.

In Fig. 1 we show the modulus-squared or the probability of the wavefunction calculated at $t=16T$. Two calculations with $x_{max}=300$ and 400 have been carried out. The two calculations yield results that are not distinguishable in the figure. These results are compared to the calculations using the split-operator method (dashed lines) with an absorber of the form $f(x)=[1+\exp(1.25x\pm350)]^{-1}$ when the boundaries are set at $x_{max}=\pm400$. Comparing the present results with those from the split-operator method, we note that the agreement is quite good for $x$ between $-150$ and 150. Note that the wavefunction obtained using the present method vanishes for $x$ less than $-250$ and $x$ greater than 250, even though the boundaries were set further out. We will come back to discuss this point later.

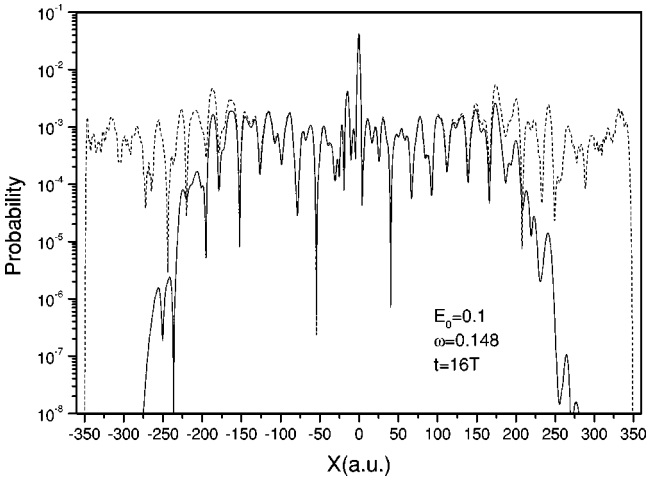


FIG. 1. Probability (or modulus squared of the wave function) vs $x$ calculated for a model 1D atom in a laser field of strength $E_0=0.1$, $\omega=0.148$, and $t=16$ T. Each calculation is confined to the boundaries defined by $-x_{max}$ and $x_{max}$. The solid line is from the present least-squares fitting method, and the dotted lines are from the split-operator method with an absorber at the boundaries (see text). The present calculations used two sets of parameters: (a) $x_{max}=300$ and $N=600$; (b) $x_{max}=400$ and $N=800$ but the results agree and are indistinguishable on the graph.

In Fig. 2 we show the normalized harmonic generation spectra. The peaks occur at the odd harmonic orders only and they are quite visible up to the 13th harmonic. The agreement between the present two calculations (solid lines and dotted lines) are quite good, and they also agree with the calculation using the split-operator method (dashed lines).

In Fig. 3 we compare the ATI spectrum calculated at $t=16.25T$. For the ATI spectrum, we have averaged over the population of the even and odd discrete states as done in Ref. [24],

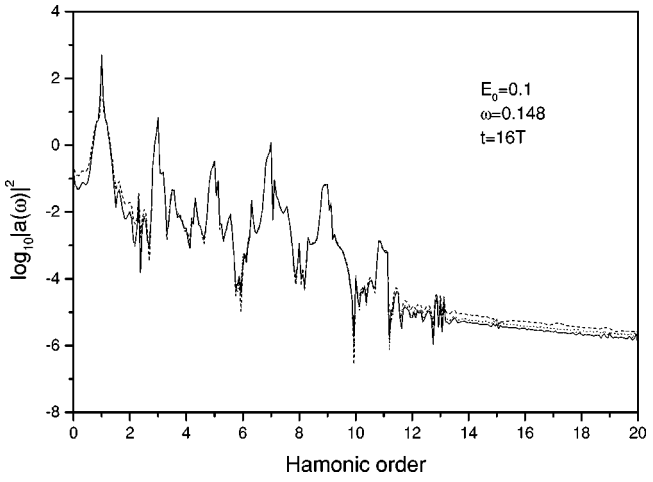


FIG. 2. Harmonic generation spectra calculated using the wave functions generated with the parameters indicated in Fig. 1. Solid line, present method, case (b) $x_{max}=400$ and $N=800$; dotted line, present method, case (a) $x_{max}=300$ and $N=600$; dashed line, split-operator method.

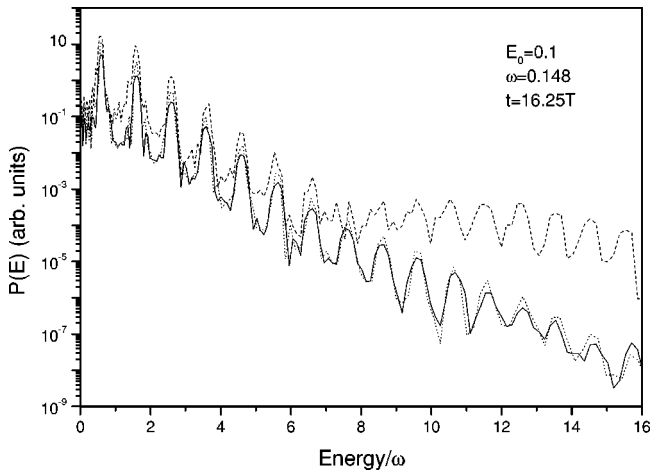


FIG. 3. ATI spectra calculated using the parameters of Fig. 1. Symbols as in Fig. 2.

$$P(\tfrac{1}{4}(E_{i-1}+E_i+E_{i+1}+E_{i+2}),t)=\frac{|c_i(t)|^2}{E_{i+1}-E_{i-1}}+\frac{|c_{i+1}(t)|^2}{E_{i+2}-E_i}. \tag{17}$$

Clearly the present two calculations give essentially identical results, and they agree very well with the split-operator method results for up to about the sixth peak. From there on the high-energy ATI peaks obtained from the split-operator methods have higher intensities than those from the present method. The discrepancy is likely due to the different methods of treating the loss of the flux (or probability) at the boundaries. Note that in the split-operator method the absorber changes the probability near the boundaries only. The present method, with the least-squares fitting, apparently removes the probabilities over a larger region near the boundaries. In Fig. 4 we show the calculated ionization probability as a function of the laser interaction time. The results from the present method (solid line) agree quite well with those from the split-operator method (dashed lines).

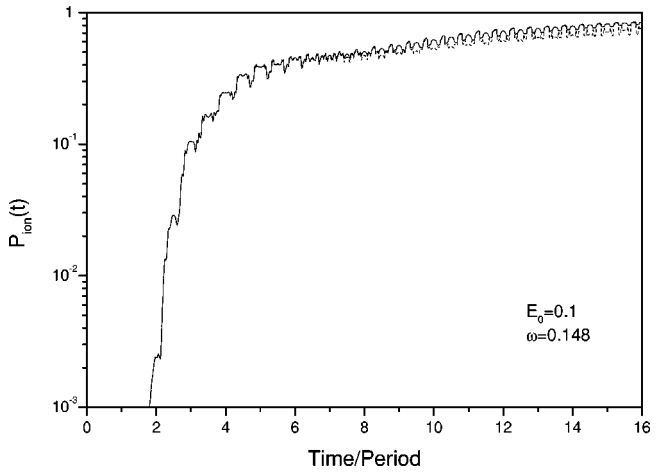


FIG. 4. Comparison of total ionization probability as a function of time calculated using the present method with $x_{max}=400$ and $N=800$ and the result from the split-operator method.

We now return to discuss the probability of the wave function shown in Fig. 1. The present method and the split-operator method give essentially identical results in the inner region, while they disagree in the outer region. The probability is much larger from the split-operator calculation. It vanishes only near the boundaries and the sharp drop to zero near the boundaries clearly is a consequence of the absorber adopted. With the absorber, one can still see the effect of interference, as evidenced by the rapid oscillation of the probabilities in the outer region in the split-operator results. These fast oscillations from the interference may be the cause of the higher ATI peaks in the higher energy region. On the other hand, the present fitting procedure removes all the higher oscillations, thus basis functions with higher eigenenergies are not populated. This explains why our calculated probabilities are smaller in the outer region and why the high-energy ATI peaks are weaker.

So far in the present calculation we did not need to introduce any absorber to remove reflections from the boundaries. However, when $x_{max}$ was chosen to be 200 a.u. we found strong interference and the results were not acceptable. The interference is similar to what one would get from using the split-operator method without the absorber. Within this smaller range, the fitting procedure was not able to remove the effect of reflection from the boundaries. Of course one can introduce absorbers into the present fitting method as well. In Fig. 5 we show the probability calculated with the present least-squares fitting method with $x_{max}=200$, one without the absorber, and the other with the absorber, where the functional form of the absorber is the same as the one used in the split-operator method. Clearly without the absorber the probability (dotted lines) oscillates rapidly showing the effect of reflection and interference. By introducing the absorber, the probability (solid line) becomes much smoother. We next compare the harmonic generation spectra obtained from calculations using $x_{max}=200$ with the absorber (dotted lines), with the results from using $x_{max}=400$ without the absorber (solid line). The results in Fig. 6 show

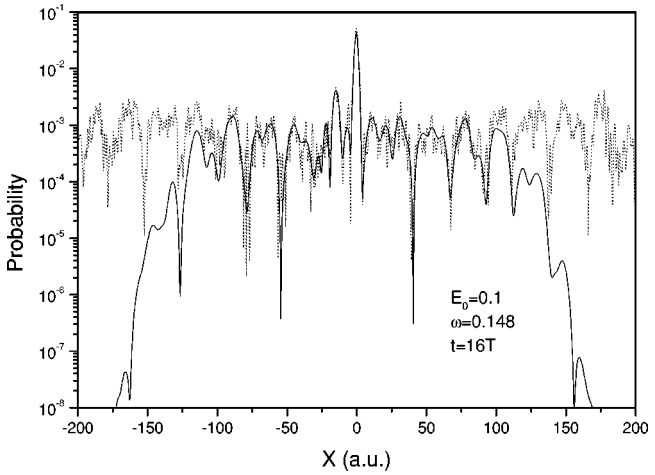


FIG. 5. The probability of the wave function calculated using boundaries at $x_{max}=200$ and $N=400$. The dashed lines are calculated without the absorber and solid line is obtained using an absorber identical to the one used in the split-operator method.

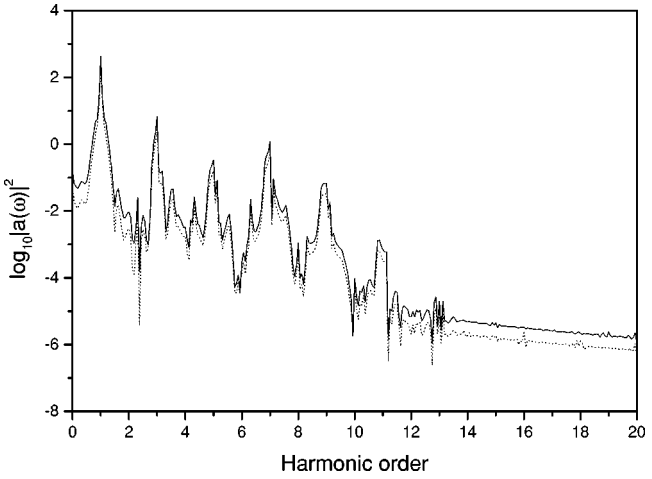


FIG. 6. Comparison of the harmonic generation spectra obtained using the present method but with different parameters. Solid line, $x_{max}=400$ and $N=800$ without the absorber; dashed lines, $x_{max}=200$ and $N=400$ with the absorber.

that the agreement is quite acceptable. Figure 7 shows the comparison for the ATI spectra from the two calculations and they again agree quite well. Thus we can use a smaller range of $x_{max}$ to achieve the same results if the absorbers were added at the boundaries.

### B. Harmonic generation for $E=0.08$ a.u. and $\omega=0.06$ a.u.

We next give another example for calculations carried out in the tunneling region where the Keldysh parameter is less than one and where ionization is dominated by the tunneling of the electron in the oscillating laser field. In Fig. 8 we show the probability distribution calculated at $t=16$ T from the present fitting procedure with $x_{max}=300$ and compare the results to the split-operator method with absorbers. Again the results agree quite well. The harmonic generation spectra, as shown in Fig. 9 also agree quite well to very high order.

## IV. SUMMARY AND DISCUSSION

In this paper we have illustrated a different method of solving the time-dependent Schrödinger equation for a one-dimensional model atom in a laser field. The method is based on the eigenfunction expansion method but the resulting time-dependent coefficients are calculated using the linear least-squares fitting procedure. In the process the wavefunctions at discrete grid points are evaluated, thus eliminating the need to calculate matrix elements involving the basis functions. We summarize what we consider the highlights of this method: (1) The choice of basis functions is very flexible. They can be tailored to particular physical systems. (2) The calculation does not require evenly spaced grid points. Thus denser mesh points can be used for the region where the atomic potential is strong while sparse mesh points can be used for the outer region where the atomic potential is essentially zero. (3) There is no need to introduce absorbers near the boundaries of the integration region. By restricting basis functions to a certain energy range, the fitting procedure removes the highly oscillating components of the the time-dependent wavefunctions to damp out the oscillations

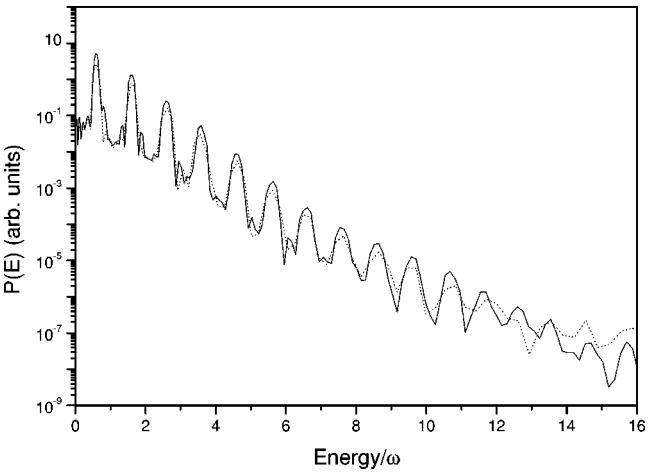


FIG. 7. The same as Fig. 6 but for the ATI spectra.

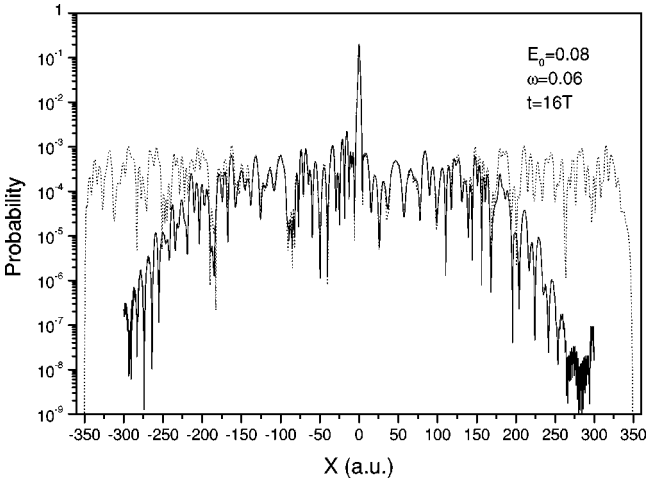


FIG. 8. Probability of the wave function calculated for the 1D model atom in a laser field with $E_0=0.08$, $\omega=0.06$, and $t=16$ T. The solid line is from the present calculation using $x_{max}=300$ and $N=600$ and the dotted lines are from the split-operator method and with an absorber.

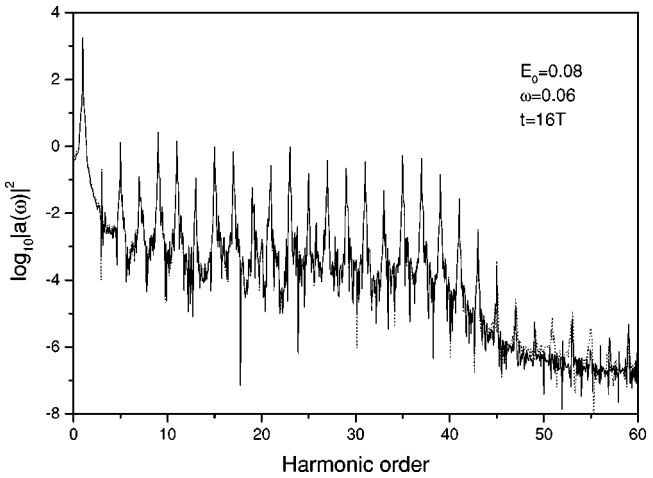


FIG. 9. The harmonic generation spectra calculated using the wave functions of Fig. 8.

due to the reflection from the boundaries. (4) From the results shown in Figs. 5–8, it appears possible to reduce the range of the ''box'' by introducing absorbers on the boundaries. This allows the use of a smaller basis set and smaller number of grid points to save computational time and memory.

In summary we have shown that the least-squares fitting procedure for solving the time-dependent equation can achieve accurate results as obtained from the split-operator method without the need of introducing absorbers. The method can be easily applied to any form of laser fields, to examine the effect of combined fields, and to study phase controls. It is also straightforward to generalize the method to three-dimensional problems. Since the control on the basis sets and the grid points is rather flexible, they can also be adjusted to simplify calculations depending on the specific physical system.

## ACKNOWLEDGMENTS

We thank Professor T. F. Jiang for many helpful discussions and for providing the split-operator method code for checking the results presented here. We also thank Dr. Emil Sidky for helping with the least-squares fitting procedure. This work was supported in part by the U.S. Department of Energy Office of Science, Office of Basic Energy Sciences, and Division of Chemical Sciences.

[1] *Atoms in Intense Fields*, Adv. At. Mol. Phys. Suppl. 1 (1992), edited by M. Gavrila.
[2] K. Burnett, V. C. Reed, and P. L. Knight, J. Phys. B **26**, 561 (1993).
[3] M. Protopapas, C. H. Keitel, and P. L. Knight, Rep. Prog. Phys. **60**, 389 (1997).
[4] S. I. Chu, Adv. At. Mol. Phys. **21**, 197 (1985).
[5] R. M. Potvliege and R. Shakeshaft, Phys. Rev. A **38**, 4597 (1988).
[6] M. R. Hermann and J. A. Fleck, Phys. Rev. A **38**, 6000 (1988).
[7] J. L. Krause, K. J. Schafter, and K. C. Kulander, Phys. Rev. A **45**, 4998 (1992).
[8] K. J. LaGattuta, J. Opt. Soc. Am. B **7**, 639 (1990).
[9] P. L. Devries, J. Opt. Soc. Am. B **7**, 517 (1990).
[10] J. H. Eberly, Q. Su, and J. Javanainen, Phys. Rev. Lett. **20**, 881 (1989).
[11] B. Sundaram and L. Armstrong,Jr., J. Opt. Soc. Am. B **7**, 414 (1990).
[12] S. Geltman, J. Phys. B **27**, 1497 (1994).
[13] Th. Mercouris, Y. Komninos, S. Dionissopoulou, and C. A. Nicolaides, Phys. Rev. A **50**, 4109 (1994).
[14] X. Tang, H. Rudolph, and P. Lambropoulos, Phys. Rev. Lett. **24**, 3269 (1990); E. Cormier and P. Lambropoulos, J. Phys. B **29**, 1667 (1996).
[15] S. M. Susskind and R. V. Jensen, Phys. Rev. A **38**, 711 (1988).
[16] Ph. Antoine, B. Piraux and A. Maquet, Phys. Rev. A **51**, R1750 (1995).
[17] L. A. Collins and A. L. Merts, J. Opt. Soc. Am. B **7**, 647 (1990).
[18] C. Raman, C. W. S. Conover, C. I. Sukenik, and P. H. Bucksbaum, Phys. Rev. Lett. **76**, 2436 (1996).
[19] T. J. Bensky, G. Haeffler, and R. R. Jones, Phys. Rev. Lett. **79**, 2018 (1997).
[20] R. Moshammer *et al.*, Phys. Rev. A **56**, 1351 (1997).
[21] M. A. Abdallah *et al.*, Phys. Rev. Lett. **81**, 3627 (1998).
[22] E. Y. Sidky and C. D. Lin, J. Phys. B **31**, 2949 (1998).
[23] T. F. Jiang and S. I. Chu, Phys. Rev. A **46**, 7322 (1992).
[24] J. Javanainen, J. H. Eberly, and Q. Su, Phys. Rev. A **38**, 3430 (1988).
[25] W. H. Press *et al.*, *Numerical Recipes in Fortran* (Cambridge University Press, Cambridge, England, 1992), pp. 665–669.
[26] J. H. Eberly, Q. Su, and J. Javanainen, J. Opt. Soc. Am. B **6**, 1289 (1989).